TWO-DIMENSIONAL MAGNETIC PHASE TRANSITION OF ULTRATHIN IRON FILMS ON Pd(100)*

C. Liu and S. D. Bader

Materials Science Division
Argonne National Laboratory
Argonne, IL 60439

CONF-891117--10

DE90 003555

Epitaxial Fe films grown on Pd(100) are used to study monolayer magnetism, critical behavior, and surface magnetic anisotropy, by means of *in-situ* surface magneto-optical Kerr-effect measurements. Auxilliary LEED-Auger observations in 10^{-11} Torr vacuum are used to characterize the (1x1) epitaxy and the layer-by-layer film-growth mode. Ferromagnetic hysteresis loops were detected for all Fe thicknesses from 0.6-4 monolayers (ML) with the T_C monotonically increasing with thickness, independent of the easy-axis orientation. The easy axis is perpendicular to the film plane below a critical thickness of 2.5 ML for 100-K film growth, and reorients in-plane above this thickness, and for all thicknesses for films grown at 300K. The temperature dependence of the magnetization was obtained from the height of the Kerr loops in the remanent state and used to extract an effective magnetization exponent ß for different film thicknesses and spin orientations. A value of ß=0.127±0.004 is reported for a 1.2-ML Fe film with perpendicular spin orientation from a log-log plot for $T>0.9T_C$, in agreement with the value of the theoretical 2-dimensional Ising critical exponent $ß_C=1/8 =0.125$.

PACS numbers: 75.70.Ak, 75.30.Gw, 75.40.Cx, 78.20Ls

* Supported by the U.S. Department of Energy, Basic Energy Sciences-Materials Sciences, Contract No. W-31-109-ENG-38.

The phase transition of a two-dimensional (2D) ferromagnet has long been a subject of interest. Exact solutions were found ~40 years ago for ideal 2D Ising models including both the short-[1] and long-range order[2] in the crystal lattice. These calculations demonstrate that the spontaneous magnetization should undergo a second-order phase transition at a Curie temperature T_C with a critical exponent β_c of 1/8. Experimental data for monolayer-range magnetic phase transitions have only been forthcoming quite recently.[3-6] Dürr, *et al.*[3] studied the system Fe/Au(100) and extracted an effective exponent ß of 0.22. This ß-value deviates from the theoretical β_c value of 1/8 and raises the question of the ability of the 2D Ising model to describe ultrathin magnetic films. However, Fe has a large solubility[7] in Au, and Au also can segregate to the surface[8] because of its low surface free energy[9] compared to that of Fe. In the present work, we study Fe/Pd(100) because it has better thermal reversibility of its magnetic properties in the monolayer (ML) and submonolayer range than Fe/Au(100). Fe/Pd(100) also exhibits perpendicular spin orientations below a critical thickness due to the surface magnetic anisotropy, and provides an example of a new phase stabilized via epitaxy. Au(100) substrates yield lattice-matched bcc Fe(100) multilayers, while Pd(100) yields body-centered tetragonal (bct) Fe(100).

The films were grown and characterized under 10^{-11} Torr ultra-high vacuum (UHV) conditions. The Pd(100) substrate was mechanically polished to a 1-μ diamond-paste finish, installed with its [110] direction aligned (horizontally) in the plane of incidence. Repeated Ar^+-sputter and 650°C-anneal cycles were applied until sharp p(1x1) low-energy electron diffraction (LEED) patterns were observed. Pd homoepitaxial evaporation at ~550°C was performed in most cases before the Fe deposition to improve the surface perfection. Fe was deposited at various substrate temperatures from 100K to 300K at a rate of ~0.6 ML/min. Epitaxial growth was obtained according to LEED observations and Auger intensity-*vs.*-deposition-time measurements. LEED patterns for Fe/Pd(100) films followed that of the substrate for the thickest films we grew, which were ~9 ML. The structural identification with the bct phase is based on our observations of epitaxy and on the quantitative LEED studies for the related system Mn/Pd(100) by Tian, *et al.*[10]

Magnetic properties were detected *in-situ* using the surface magneto-optical Kerr-effect (SMOKE) technique as previously reported.[11] SMOKE is used to monitor the in-plane and perpendicular magnetization components, via sequential longitudinal and polar Kerr measurements, respectively. Magnetic hysteresis curves are generated by sweeping the magnetic field H and detecting the change in intensity of the reflected light (wavelength = 6328Å) after passage through the UHV window and a polarizing analyzer crystal. The height of the hysteresis loop is referred to as the Kerr intensity, which is proportional to the Kerr rotation and to the magnetization of the sample. The sample temperature was measured with a chromel-alumel thermocouple spot-welded to the sample about 3 mm away from the laser-illuminated area. Magnetic phase transitions were studied by slowly changing the sample temperature and monitoring the height of the hysteresis loops in the remanent state (H=0) ~0.3s after pulsing the magnetic field to sequentially saturate the magnetization in opposite directions.

Figure 1 shows the thickness dependence of the remanent Kerr intensity for Fe/Pd(100) grown and measured at (a) ~300K and (b) ~100K. The easy axis of magnetization depends on the growth temperature. Films grown at ~300K have in-plane easy axes, where only longitudinal Kerr-effect hysteresis loops were detected. Films grown at ~100K have vertical easy axes for film thicknesses less than ~2.5 ML; the easy axis reorients in-plane for thicker films, similar to the Fe/Cu(100) case.[11] Also, films grown at ~300K retain their in-plane easy axes when they are cooled to ~100K, and those <2 ML grown at ~100K do not change their vertical easy axes up to T_C. The growth-temperature boundary between the two spin orientations is ~270K, and depends slightly on the substrate surface quality. (The boundary occurs at ~290K for substrates that have not been homoepitaxially smoothed.) The structural basis of the growth-temperature-dependent anisotropy of ultrathin films is not clear at present.

The temperature-dependence of the normalized Kerr intensities is shown in Fig. 2. Figure 2(a) is for films grown at ~300K with in-plane easy axes, so only the longitudinal SMOKE signals show hysteresis. The data were taken from the measured hysteresis loops. Figure 2(b) is for films grown at ~100K with vertical easy axes, as measured in the polar SMOKE configuration with the remanent Kerr intensities directly recorded as the sample temperature was slowly varied. All films undergo second-order magnetic phase transitions with thickness-dependent T_C values. The transitions are thermally reversible, as shown by the overlap of the warming- and cooling-curve data sets. The hysteresis loops (not shown) were also unaltered after the temperature-dependence measurements were made, in sharp contrast to the behavior of monolayer thicknesses of Fe/Cu(100) [Ref. 11] and Fe/Au(100) [Ref. 12]. The favorable thermal-reversibility characteristic is attributed to the higher surface free energy σ of Pd compared to that of Cu and Au, where σ_{Pd}= 2.10 J/m^2, σ_{Cu}= 1.85 J/m^2, and σ_{Au}= 1.55J/m^2 compare to the tabulated[9] value for bcc Fe of 2.55 J/m^2.

To study the magnetic behavior near T_C we adopt the standard methodology as used in Ref. 3 and assume that the transition follows a power law whereby the magnetization M and the Kerr intensity are proportional to $(1 - T/T_C)^{\beta}$ below a parametrized value of T_C. The effective exponent ß is then deduced by choosing a T_C value that maximizes the range of a straight-line fit in a log M-*vs*.-log $(1 - T/T_C)$ plot.[13] Figure 3 shows log-log plots for the indicated data from Fig. 2. The ß values obtained from the slopes of the straight lines are all close to the theoretical β_c-value of 0.125 for a 2D Ising model.[1,2] In particular, the 1.2-ML data set, which has the most densely spaced points, yields ß = 0.127 ± 0.004. These results conform to the expectation that a Heisenberg system with even arbitrarily small anisotropy yields an Ising-like transition in 2D.[14]

The tails on the high-temperature side of the transitions shown in Fig. 2 are indicative of finite-size effects, as pointed out in Ref. 3. Landau has calculated M(T) for finite-size Ising square lattices with both free-edge and periodic boundary conditions.[15] His calculations in both cases show that the transitions are rounded and that there are pronounced tails extending above T_C. The rounding effect gives the appearance of effective ß-values that are greater than the β_c-value for the infinite 2D film. This trend in ß-values can explain the experimentally-determined drift in ß from 0.13 to 0.16 on

going from the 1.2- to the 0.6-ML film. The 1.2-ML film is expected to be continuous, and, therefore, to better simulate an ideal film than the 0.6-ML film, which should consist of rather discontinuous 2D islands. Another important aspect of the analysis of the experimental transition widths involves the influence of the induced magnetic moments of the interfacial Pd, as predicted theoretically.[16] This issue will be treated in a separate publication.[17]

It is of interest to observe the evolution of the hysteresis loops through the transition. The data in Fig. 2(b) were taken in the remanent state without generating the loops. Figure 4, however, shows polar loops for a ~1.5-ML-thick film grown at 240K and measured at the indicated temperatures. Note that even for this relatively-high growth temperature the vertical easy axes are still stable. The parametrized T_C-value is ~450K. The remanence persists even though the field itself can further broaden the transition.

Figure 5 shows the thickness dependence of T_C as determined from the fitting procedure. It is of interest to note that the T_C-*vs.*-thickness data follow a monotonic curve for both the in-plane and vertical easy-axis orientations. There is a rapid change in the T_C values in the monolayer and submonolayer region and a more gradual change for the thicker films. The trend is in agreement with that of Binder and Hohenberg obtained from Monte-Carlo calculations for free-standing Ising films.[14] In Fig. 5 their results are shown as small crosses, scaled to our 3-ML film and connected by a dashed line. The agreement between experiment and calculation is remarkably good. A recently predicted T_C minimum in the critical thickness region (2-3 ML in our case) is not found.[18] We do find, however, in this region that the easy axes of films grown at 100K reorient in-plane as the temperature increases.

In conclusion, a 2D magnetic phase transition has been characterized for the Fe/Pd(100) ultrathin-film system. The magnetization exponent ß is found to be 0.127 ± 0.004 for a 1.2-ML Fe film that possesses vertical spin orientations. This conforms to theoretical expectation for 2D Ising critical behavior, as anticipated for 2D Heisenberg systems with anisotropy. The easy-axis characteristics and T_C trend with thickness have also been systematized.

This work was supported by the U.S. Department of Energy, BES-Materials Sciences, under contract #W-31-109-ENG-38.

References:

1. L. Onsager, Phys. Rev. **65**, 117 (1944); B. Kaufman and L. Onsager, Phys. Rev. **76**, 1244 (1949).
2. C. N. Yang, Phys. Rev. **85**, 808 (1952).
3. W. Dürr, M. Taborelli, O. Paul, R. Germar, W. Gudat, D. Pescia and M. Landolt, Phys. Rev. Lett. **62**, 206 (1989).
4. C. Rau and M. Robert, Phys. Rev. Lett. **58**, 2714 (1987).
5. C. Rau, G. Xing, and M. Robert, J. Vac. Sci. Technol. A **6**, 579 (1988).
6. M. Farle and K. Baberschke, Phys. Rev. Lett. **58**, 511 (1987).
7. See, e.g., M. Hansen, **Constitution of Binary Alloys**, (McGraw-Hill, New York, 1958), p. 203.
8. E. R. Moog and S. D. Bader, Superlatt. Microstruct. **1**, 543 (1985).
9. A. R. Miedema, Z. Metallkde, 69, 287 (1978); and J. C. Hamilton, Phys. Rev. Lett. **42**, 989 (1979).
10. D. Tian, S. C. Wu, F. Jona, and P. M. Marcus, Solid State Commun. **70**,199 (1989).
11. C. Liu, E. R. Moog, and S. D. Bader, Phys. Rev. Lett. **60**, 2422 (1988); J. Appl. Phys. **64**, 5325 (1988).
12. C. Liu and S. D. Bader, J. Vac. Sci. Tech., accepted.
13. D. L. Connelly, J. S. Loomis, and D. E. Mapother, Phys. Rev. B **3**, 924 (1971).
14. K. Binder and P. C. Hohenberg, IEEE Trans. on Magnetics, **MAG-12**, 66 (1976).
15. D. P. Landau, Phys. Rev. **B13**, 2997 (1976).
16. S. Blügel, M. Weinert, and P. H. Dederichs, Phys. Rev. Lett. **60**, 1077, (1988); and in **Proceedings of the 18th Annual International Symposium on Electronic Structure of Solids**, edited by P. Ziesche (TU Dresden, 1988), p. 101.
17. C. Liu, E. Ratner, and S. D. Bader, to be published.
18. M. Bander and D. L. Mills, Phys. Rev. B **38**, 12015 (1988).

Figure Captions:

Fig. 1. Fe-film-thickness dependence of the Kerr intensity for Fe/Pd(100) grown and measured at (a) ~300K and (b) ~100K. The lines through the data are guides to the eye.

Fig. 2. Temperature dependence of the normalized Kerr intensity for Fe/Pd(100) films grown at (a) ~300K and (b) ~100K. Note the reversibility for warming and cooling curves.

Fig. 3. Log-log plots of the temperature dependence of the Kerr-intensity data for Fe/Pd(100) from Fig. 2, along with the values of the effective magnetization exponent ß. The data sets are offset from each other for clarity.

Fig. 4. Polar hysteresis loops for a ~1.5-ML Fe film grown at 240K and measured at the indicated temperatures.

Fig. 5. Thickness dependence of T_C for in-plane (triangles) and vertical (squares) spin orientations. The dashed curve connects the results of the Monte-Carlo calculations of Ref. 14 as scaled to experiment at 3 ML.

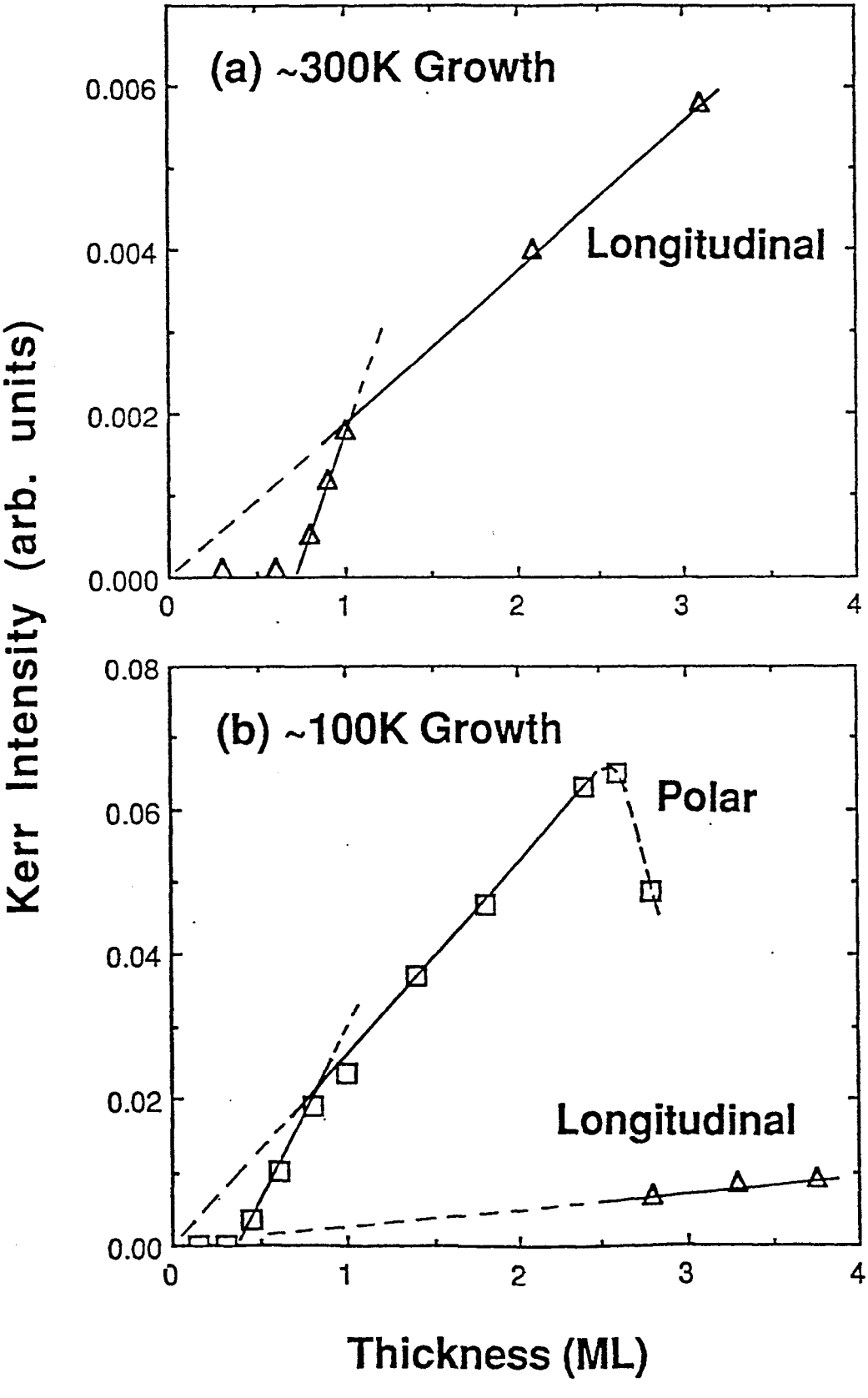
(a) ~300K Growth
Longitudinal
0.006
0.004
0.002
0.000
0
1
2
3
4
(b) ~100K Growth
Polar
Longitudinal
0.08
0.06
0.04
0.02
0.00
Kerr Intensity (arb. units)
Thickness (ML)

Fig. 1

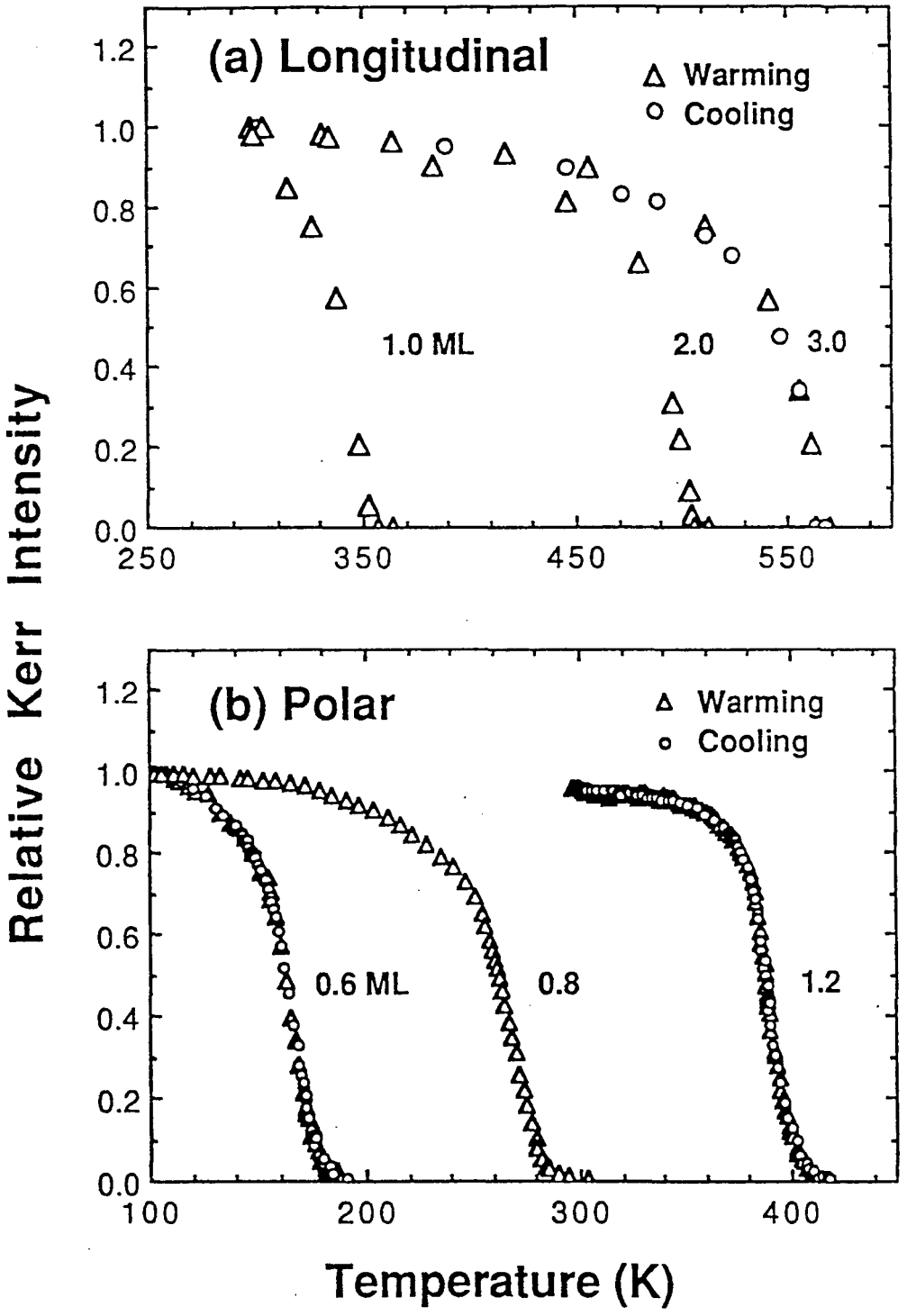
(a) Longitudinal
Warming
Cooling
1.0 ML
2.0
3.0
(b) Polar
Warming
Cooling
0.6 ML
0.8
1.2
Relative Kerr Intensity
Temperature (K)

Fig. 2

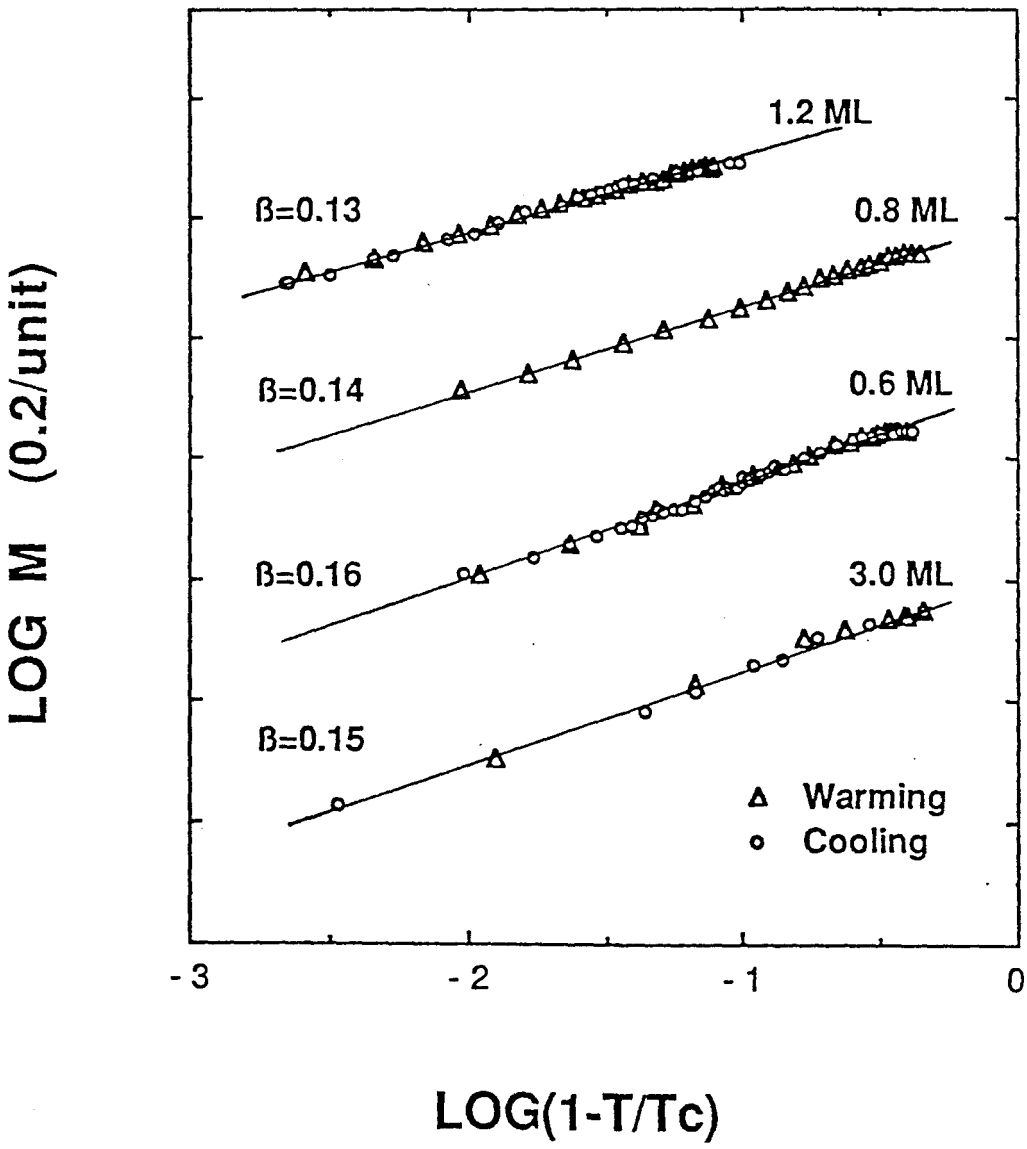
1.2 ML
ß=0.13
0.8 ML
ß=0.14
0.6 ML
ß=0.16
3.0 ML
ß=0.15
Warming
Cooling
- 3
- 2
- 1
0
LOG M (0.2/unit)
LOG(1-T/Tc)

Fig. 3

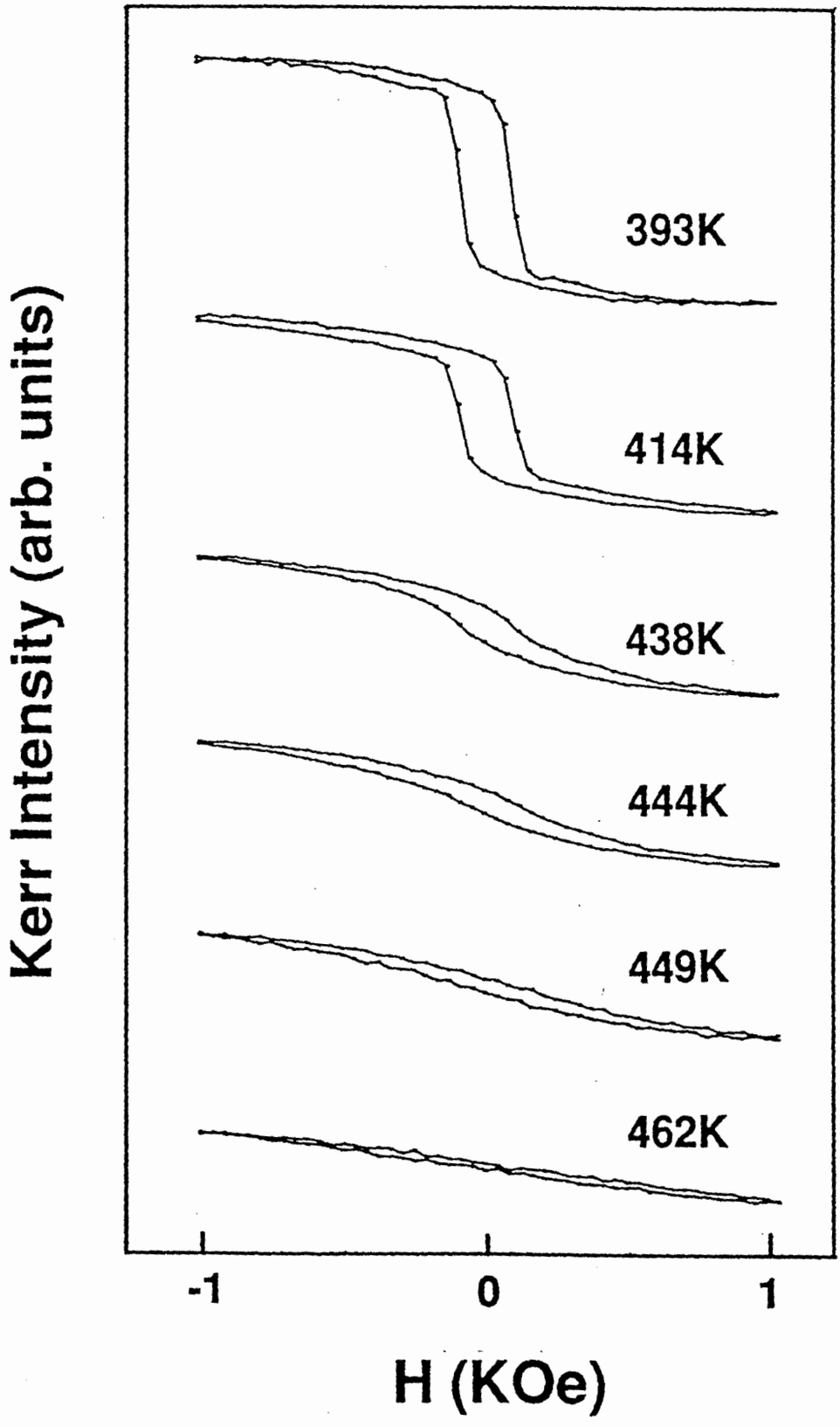
Kerr Intensity (arb. units)
393K
414K
438K
444K
449K
462K
-1
0
1
H (KOe)

Fig. 4

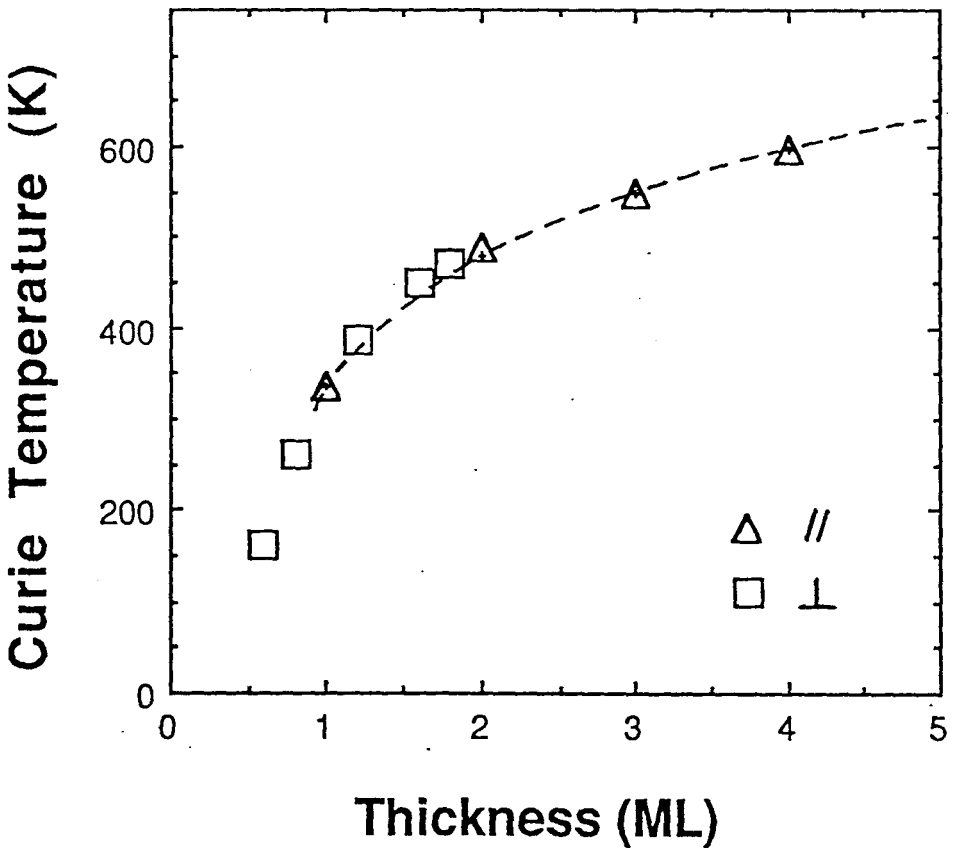

Fig. 5